Published in final edited form as:

Oncogene. 2015 May 28; 34(22): 2856–2866. doi:10.1038/onc.2014.233.

Lineage-specific *RUNX3* hypomethylation marks the preneoplastic immune component of gastric cancer

B Kurklu[1,2], **RH Whitehead**[2], **EK Ong**[1], **T Minamoto**[3], **JG Fox**[4], **JR Mann**[1,5], **LM Judd**[1,2], **AS Giraud**[1,2,6], and **TR Menheniott**[1,2,6]

[1]Infection and Immunity, Murdoch Children's Research Institute, Royal Children's Hospital, Parkville, Victoria, Australia

[2]Department of Paediatrics, University of Melbourne, Melbourne, Victoria, Australia

[3]Division of Translational and Clinical Oncology, Cancer Research Institute, Kanazawa University, Kanazawa, Japan

[4]Division of Comparative Medicine, Department of Biological Engineering, Massachusetts Institute of Technology, Cambridge, MA, USA

[5]Department of Zoology, University of Melbourne, Melbourne, Victoria, Australia

Abstract

Runt domain transcription factor 3 (*RUNX3*) is widely regarded as a tumour-suppressor gene inactivated by DNA hypermethylation of its canonical CpG (cytidine-phosphate-guanidine) island (CGI) promoter in gastric cancer (GC). Absence of *RUNX3* expression from normal gastric epithelial cells (GECs), the progenitors to GC, coupled with frequent *RUNX3* overexpression in GC progression, challenge this longstanding paradigm. However, epigenetic models to better describe *RUNX3* deregulation in GC have not emerged. Here, we identify lineage-specific DNA methylation at an alternate, non-CGI promoter (P1) as a new mechanism of *RUNX3* epigenetic control. In normal GECs, P1 was hypermethylated and repressed, whereas in immune lineages P1 was hypomethylated and widely expressed. In human GC development, we detected aberrant P1 hypomethylation signatures associated with the early inflammatory, preneoplastic and tumour stages. Aberrant P1 hypomethylation was fully recapitulated in mouse models of gastric inflammation and tumorigenesis. Cell sorting showed that P1 hypomethylation reflects altered cell-type composition of the gastric epithelium/tumour microenvironment caused by immune cell recruitment, not methylation loss. Finally, via long-term culture of gastric tumour epithelium, we

Correspondence: Dr TR Menheniott, Infection and Immunity, Murdoch Children's Research Institute, Royal Children's Hospital, Parkville, Victoria 3052, Australia. treve.menheniott@mcri.edu.au.

[6]These authors contributed equally to this work.

CONFLICT OF INTEREST

The authors declare no conflict of interest.

AUTHOR CONTRIBUTIONS

TRM, ASG, LMJ and JRM conceived, designed and led the study. BK, TRM, EK and RHW performed the experiments. BK and TRM analysed the data. TM and JGF contributed reagents and materials. TRM and BK wrote the manuscript. TRM, ASG, LMJ and JRM edited and revised the manuscript. All authors approved the final version of the manuscript before submission

Supplementary Information accompanies this paper on the Oncogene website (http://www.nature.com/onc)

revealed that *de novo* methylation of the *RUNX3* canonical CGI promoter is a bystander effect of oncogenic immortalization and not likely causal in GC pathogenesis as previously argued. We propose a new model of *RUNX3* epigenetic control in cancer, based on immune-specific, non-CGI promoter hypomethylation. This novel epigenetic signature may have utility in early detection of GC and possibly other epithelial cancers with premalignant immune involvement.

INTRODUCTION

Gastric cancer (GC) has the second highest rate of cancer-related mortality worldwide, accounting for >700 000 deaths annually.[1] Late diagnosis is a major challenge to GC management, with disease presentation typical at advanced stages when treatment is ineffective and prognosis is poor.[2] Chronic inflammation after infection with *Helicobacter pylori* is a primary risk factor for the most common or 'intestinal-type' GC,[3] but definitive mechanisms remain elusive. GC is believed to be of epithelial origin, deriving from gastric epithelial cells (GECs) or their progenitors.[4,5] Elucidation of molecular events underlying the inflammation-related preneoplastic transformation of GECs[3] will be critical for the advancement of GC management, allowing earlier disease detection and improved survival.

Aberrant DNA methylation is one of the earliest molecular alterations in cancer and has been linked to GC pathogenesis.[6,7] Hypermethylated sequences become hypomethylated on a global scale. Conversely, unmethylated CpG (cytidine-phosphate-guanidine) island (CGI) promoters, including those of some tumour-suppressor genes (TSGs), become hypermethylated leading to their repression.[8] Hypermethylation of TSGs has been traditionally viewed as a persuasive mechanism of cancer pathogenesis, as well as providing a target for cancer detection.[9] Nonetheless, recent evidence that *de novo* hypermethylation in cancer mostly affects CGI promoters already repressed in normal tissues argues that methylation is not always required for their repression and therefore is not necessarily a driver of cancer.[10] Cell-type composition of the tumour microenvironment has gained attention as an alternative influence on cancer methylation profiles.[11] In this context, CpG-depleted or 'non-CGI' promoters, which show considerable variation in lineage-specific methylation, may offer complementary clinical utility to CGI promoters.[12,13] Indeed, the prognostic value of methylation signatures corresponding to non-neoplastic tumour lineages, such as cancer-associated fibroblasts or cytolytic T-lymphocytes, has recently been demonstrated.[14,15]

Runt domain transcription factor 3 (RUNX3) belongs to the family of conserved 'runt-domain' transcription factors that have diverse roles in hematopoiesis, neurogenesis and skeletal development.[16–18] *RUNX3* transcription initiates from two *cis*-regulatory regions designated the P1 (distal) and P2 (proximal) promoters. Expressed predominantly in hematopoietic lineages, RUNX3 regulates several aspects of immune function, including T-cell differentiation,[19,20] dendritic cell (DC) maturation[21] and natural killer (NK) cell activation.[22,23] In contrast to these definitive immune roles, the *RUNX3* locus (located on human chromosome 1p36.1) has been controversially linked to a TSG function in GC. In 2002, Li *et al*.[24] proposed that *RUNX3* inactivation via hypermethylation of a large CGI overlapping its P2 promoter is a pivotal event in GC pathogenesis. Subsequent studies have

confirmed the association of *RUNX3* P2 hypermethylation with GC incidence (reviewed in Fan *et al.*[25] and Subramaniam *et al.*[26]). However, fresh evidence that *RUNX3* is never expressed in the normal GEC from which GC originates[27] casts doubt not only on its proposed TSG function, but also on the role of P2 methylation in RUNX3 silencing and its associated utility as a functional marker of GC. Limitations of this widely disseminated epigenetic model[24] are further compounded by paradoxical observations of *RUNX3* overexpression in GC and other cancers[28–30] where P2 is reportedly hypermethylated.[31] Although *RUNX3* continues to feature in the literature, models to better explain its deregulation in cancer have not emerged. With its TSG function now disputed,[27] unravelling the inconsistencies of *RUNX3* epigenetic control in GC will lead to an improved understanding of its broader role in cancer biology.

In focussing exclusively on the mechanistic importance of P2 methylation, researchers have overlooked a role for the alternate 'non-CGI' *RUNX3* P1 promoter. Here we address this gap in understanding, showing that lineage-specific P1 methylation constitutes a novel and unexpected mechanism of *RUNX3* epigenetic control in GC. We find that, in normal GEC, P1 is strongly hypermethylated and repressed. By striking contrast, in immune lineages, P1 is hypomethylated and widely expressed. Through studies of human and mouse GC progression, we uncover a preneoplastic P1 hypomethylation signature reflecting altered cell-type composition of the gastric epithelium/tumour microenvironment via immune cell infiltration. Finally, we reveal that *de novo* methylation of the P2 CGI promoter in GEC, argued previously as a driver of GC pathogenesis, arises as a bystander effect of oncogenic immortalization and is unlikely to exert any significant impact on GC progression. These results delineate a novel, more parsimonious model of *RUNX3* epigenetic control with emphasis on lineage-specific P1 methylation as a marker of preneoplastic tissue remodelling. The strong translational relevance of our findings to GC, and potential application to other epithelial cancers of inflammatory provenance, is discussed.

RESULTS

RUNX3 P1 hypomethylation correlates with human GC progression

To date, all *RUNX3* methylation studies have targeted the CGI overlapping the P2 promoter, but none have interrogated P1 methylation in GC (Figure 1a). The P1 sequence falls short of the minimum CpG density criteria to qualify as a CGI (CpG observed/expected ratio >40.6; >200bp[32]) and is therefore 'non-CGI'-associated. In contrast to CGI promoters that generally resist methylation, non-CGI promoters are very likely to be regulated by methylation if CpG dinucleotides are present.[12,33] Indeed, this is the case for the human and mouse P1 sequences (Supplementary Figure S1). We therefore investigated *RUNX3* P1 expression and methylation in human gastric epithelial tissue collected from individuals displaying early-, intermediate- or late-stage intestinal-type GC development: *H. pylori*-infected/gastritis,[34] intestinal metaplasia (IM) and GC, respectively,[6] together with normal (disease-free) controls (Figure 1b). Quantitative reverse transcriptase–PCR (QRT–PCR) revealed increased total *RUNX3* mRNA expression in *H. pylori*-infected (4.05 ± 0.60-fold; $P < 0.001$), IM (8.47 ± 3.04-fold; $P < 0.01$) and GC (2.54 ± 0.73-fold; $P < 0.01$) tissues relative to normal controls (Figure 1c). Specific measurement of P1 mRNA similarly

revealed increased expression in *H. pylori*-infected (8.77 ± 1.74-fold; $P < 0.001$) but not in IM or GC tissues. The high GC content of the P2 transcript 5′ leader exon precluded its direct interrogation by QRT–PCR. These results show increased *RUNX3* P1 expression, particularly during preneoplastic stages of GC. We next examined *RUNX3* P1 methylation levels using Sequenom EpiTYPER assays. EpiTYPER quantifies the ratio of methylated to unmethylated cytosines at individual CpG dinucleotides at specific loci.[35] Although P1 hypermethylation predominated in normal gastric epithelial tissues, a P1 hypomethylation signature was significantly associated with *H. pylori*-positive, IM and GC tissues. Consistent with its CGI status, P2 remained unmethylated in *H. pylori*-infected and IM preneoplastic tissues, showing modestly increased methylation only in a subset of tumours but not exceeding 15% (that is, methylation ratio 0.15) of strands in any individual tumour (Figure 1d). Hierarchical clustering showed a clear association of P1 hypomethylation with early inflammatory, preneoplastic and tumour stages of GC. Conversely, P2 was less vulnerable to epigenetic perturbation, showing weak hypermethylation in a subset of tumours (Figure 1e). *RUNX3* P1 and P2 are thus oppositely methylated in normal gastric tissue, respectively showing uniform early loss and variable late gain of methylation in GC progression. These results identify *RUNX3* P1 hypomethylation as a novel epigenetic signature with potential utility in GC risk prediction.

Conserved *Runx3* P1 hypomethylation following *H. pylori* infection, genetic induction of gastric inflammation or tumorigenesis in mice

Human and mouse *RUNX3/Runx3* are highly conserved with respect to their genomic organization, dual promoter structure (Figure 2a) and tissue expression profile. Therefore, mouse genetic and infection models recapitulating *H. pylori*-related preneoplastic and tumorigenic stages of human GC progression (Figure 2b), offered the most stringent approach to pinpoint the origin and significance of *RUNX3* P1 hypomethylation *in vivo.* Accordingly, we first determined *Runx3* transcription and methylation in stomachs of C57BL6 (wild type; WT) mice infected with mouse-adapted *H. pylori* SS1 for either 3- or 12 months. QRT–PCR showed that P1 and P2 transcripts were progressively upregulated in 3-month (4.10 ± 1.08; $P = 0.036$ and 12.58 ± 3.00; $P = 0.008$) and 12-month (8.22 ± 1.43-fold; $P = 0.005$ and 66.59 ± 12.28-fold; $P < 0.001$) infected mice compared with uninfected littermate controls (Figure 2c). Similar to our observations in *H. pylori*-infected humans, aberrant P1 hypomethylation was evident in *H. pylori*-infected mice, showing progression from a moderate to a strong signature in 3- and 12-month infected mice, respectively. Conversely, P2 methylation was unaltered with *H. pylori* infection (Figures 2d and e). To discern effects of *H. pylori*-dependent inflammation versus bacterial presence on P1 hypomethylation, we utilized transgenic mice with stomach-specific overexpression of the pro-inflammatory cytokine, gmcsf, (*gmcsf*^{Tg}). *Gmcsf*^{Tg} mice develop spontaneous gastric inflammation independently of *H. pylori* infection.[36] *Runx3* P1 transcripts were upregulated (2.58 ± 0.31-fold; $P < 0.01$) in *gmcsf*^{Tg} compared with WT stomachs (Figure 2c) and correlated with P1 hypomethylation (Figures 2d and e). P2 was not differentially expressed or methylated (Figures 2c and e). Therefore P1 hypomethylation correlates with gastric inflammation, not with *H. pylori's* presence *per se.* To determine whether P1 hypomethylation persists later in GC progression, we utilized the *gp130*$^{F/F}$ GC model.[37] *Gp130*$^{F/F}$ mice develop tumours of the distal stomach with similar histopathology to human

GC. Though epithelial in origin, *gp130*$^{F/F}$ tumours are strongly infiltrated by cells of the innate and adaptive immune system. Increased P1 transcription (9 ± 1.46-fold; $P < 0.05$) (Figure 2b) and P1 hypomethylation were clearly correlated in *gp130*$^{F/F}$ tumours (Figures 2c and d), further supporting a link with gastric inflammation. Conversely, P2 transcription was increased (23.19 ± 6.10-fold; $P<0.01$) independently of its methylation status (Figures 2b and d). These results show that aberrant *RUNX3* P1 hypomethylation is a conserved, inflammation-associated process correlating with the preneoplastic and tumorigenic stages of GC.

RUNX3 localizes to infiltrating immune cells and not to epithelial cells in gastric preneoplasia and cancer

RUNX3 was localized in *H. pylori*-infected ($n = 16$) and uninfected ($n= 6$) human gastric tissues by immunohistochemistry. RUNX3-specific staining was detected in nuclei of immune cells infiltrating the lamina propria of *H. pylori*-infected but was not detected in uninfected tissues (Figure 3a). RUNX3 was not detected in GECs of infected or uninfected individuals. We similarly analysed the stomachs from *gmcsf*^{Tg} and *gp*130$^{F/F}$ mice. In *gmcsf*^{Tg} mice, RUNX3-specific staining localized to the nuclei of immune cells infiltrating the gastric epithelium but was not detected in GECs (Figure 3b). Similarly, in *gp130*$^{F/F}$ mice, RUNX3 was detected in immune cells infiltrating lamina propria of antral tumours and in submucosal lymphoid pockets but was not detected in GECs (Figure 3c). Earlier work showed absence of RUNX3 in normal mouse intestinal epithelium;[27] however, our results make the novel and critical distinction of showing absence of RUNX3 in normal, preneoplastic and tumour gastric epithelium in both humans as well as in mice. Therefore, *RUNX3* overexpression in gastric preneoplasia and cancer is likely dependent on immune cell recruitment.

Differential *Runx3* P1 methylation in GECs and immune lineages

Runx3 is known to be highly expressed in immune lineages (Supplementary Figure S2). Localization of gastric RUNX3 to infiltrating immune cells suggested that altered P1 methylation could similarly reflect immune cell recruitment. To address this, we isolated immune lineages known to have high Runx3 expression: NK1.1+CD3− NK cells, CD8+ T-cells, CD11c+ DCs, or low/absent Runx3 expression: CD11b+ macrophages, Gr1+ neutrophils, and CD45R+ B-cells from the spleens of WT mice by fluorescence-activated cell sorting (FACS) (Figure 4a; Supplementary Figure S3) and characterized their *Runx3* mRNA and methylation profiles relative to primary GECs. *Runx3* P1 transcripts were detected in all immune cell types except B-cells, being most abundant in NK cells, CD8+ T-cells and DCs. P2 transcripts were abundant only in NK cells, showing modest levels in other lineages and were absent in GECs (Figure 4b). Strikingly, P1 was hypomethylated in all immune cell types irrespective of their *Runx3* expression level. This suggests that P1 hypomethylation is permissive but not sufficient for transcription. Conversely, P1 was hypermethylated in primary GECs and mouse embryonic fibroblasts, which lack *Runx3* expression (Figure 4c). By reference to the public domain transcriptome data, mast cells (MCs) were noted for abundant *Runx3* mRNA expression (Supplementary Figure S2) but have otherwise not been formally described to express *Runx3.* Analysis of spleen-derived, c-

kit/CD117+FcεR1 + MCs (Figure 4a) confirmed *Runx3* P1 hypomethylation and transcription at similar levels to CD8+ T-cells (Figures 4b and c).

Our results showing universal P1 hypomethylation in immune cells suggested that its specific epigenetic state might originate before, or during, hematopoiesis. To address this question, we tracked P1 methylation levels during MC differentiation from mouse bone marrow stem cells (BMSCs) cultured with interleukin (IL)-3. Correct MC differentiation was verified by the acquisition of a c-kit/CD117+FcεR1α+ surface phenotype (Figure 4d) and induction of *carboxypeptidase* (*Cpa3*) mRNA (Supplementary Figure S3). Bone marrow-derived MCs showed strong induction of *Runx3* P1 mRNA relative to BMSCs showing only marginal expression, while P1 was equivalently hypomethylated in BMSCs and differentiated MCs (Figures 4e and f). Similar results were obtained in bone marrow-derived DCs (B Kurklu, unpublished data). These results argue that immune-specific P1 hypomethylation is inherited from BMSCs, further suggesting the existence of a developmental mechanism that protects P1 against *de novo* methylation in certain contexts.

Immune cell recruitment accounts for *Runx3* P1 hypomethylation in gastric epithelial tumours

We next examined P1 methylation in GECs and immune cells isolated directly from *gp130*$^{F/F}$ gastric tumours. Dissected tumours were non-enzymatically disaggregated, and the following cell types were recovered by FACS: e-cadherin+ GECs, CD8+ T cells, and CD11c+ DCs (Figure 5a). EpiTYPER analysis of these tumour cell fractions revealed that P1 hypomethylated alleles were enriched in CD8+ T-cells and CD11c+ DCs. Conversely, P1 hypermethylated alleles were enriched in e-cadherin+ GECs. P2 was unmethylated in tumour-derived immune cells and GECs (Figures 5b and c). That is, hypomethylated P1 alleles reside predominantly within the immune, but not the epithelial component of gastric tumours, supporting immune cell recruitment as a key mechanism underlying a *RUNX3* P1 hypomethylation signature in GC progression.

Runx3 P2 hypermethylation triggered by immortalization of GECs

RUNX3 P2 hypermethylation clearly has no direct role in *RUNX3* repression or as an autonomous driver of GC; however, its significance remains unexplained. Cancer-related *de novo* methylation targets repressed CGI promoters,[10,38] and this global deregulation of methylation may arise as an effect of cellular immortalization.[38] Immortalized cell lines often show more extensive CGI hypermethylation than corresponding primary tumours.[39] Accordingly, we compared P2 methylation levels in immortal human GC cell lines and primary GC tissues. Five out of the six cell lines showed near complete (>90%) P2 hypermethylation (Figure 6a) contrasting with much lower levels (<15%) in primary GC tumour tissues. The single exception was the slow growing NCI-N87 line, which showed only marginally increased P2 methylation levels. P1 methylation levels were similar in both normal, tumour and cell lines. These results reveal a specific correlation between hypermethylation of the P2 CGI and GEC immortalization. To explore this concept, we next quantitated P2 methylation levels in mouse GECs both before and after their immortalization *in vitro*. Immortalization, defined as the inappropriate acquisition of indefinite proliferation, was induced by serial passage of cultured primary GECs isolated

from *gp130*$^{F/F}$ gastric tumours (Figure 6b). We cloned five GEC lines showing key features of an immortalized phenotype, including a high level of aneuploidy and the capacity to proliferate indefinitely in culture. Additionally, two of the lines displayed anchorage-independent growth in soft agar, yet all of the lines retained expression of key epithelial marker proteins, including cytokeratin (Krt)8 (Figures 6c and d; Supplementary Table S1). Though derived from primary GECs lacking P2 methylation, four of the five GEC lines had acquired high-level P2 hypermethylation after immortalization (Figure 6e). P2 methylation levels were the highest in the fastest growing lines (clones1, 3 and 5), whereas only minor gains in methylation were observed in the slowest growing line (clone 2). Conversely, P1 methylation in the immortal GECs was unperturbed relative to normal GECs (Figure 6e), consistent with evidence that *de novo* methylation in epithelial carcinogenesis may specifically target repressed CGI promoters. Therefore, P2 hypermethylation can be induced during GEC immortalization, likely in concert with *de novo* hypermethylation of other CGI promoters on a global scale. The over-representation of P2 hypermethylation among GC cell lines argues that CGI hypermethylated GEC clones may have a growth advantage, resulting in their preferential expansion in culture.

DISCUSSION

This work is the first to reveal a role for *RUNX3* P1 promoter methylation in regulating lineage-specific *RUNX3* transcription in the stomach. We specifically showed that P1 methylation is established differently in GEC and immune cells and that increased recruitment of the latter underlies aberrant P1 hypomethylation in GC progression. Finally, we showed that *de novo* methylation of the P2 CGI promoter in GEC/tumour cells, argued previously as a driver of GC progression, likely arises as a bystander effect of oncogenic immortalization and is unlikely to have a causal role in the disease. We surmise that an *in vitro* growth advantage, associated with global CGI promoter hypermethylation, leads to an over-representation of hypermethylated P2 alleles in immortal GC cell lines. Our novel findings are summarized in Figure 7.

More than a decade has passed since Li *et al.*[24] initially described *RUNX3* as a TSG repressed by P2 hypermethylation in GC. Then recognized as a significant advance, the findings engendered a long-standing paradigm of gastric tumorigenesis via TSG epigenetic loss. Frequent P2 hypermethylation in GC and other cancers remains undoubted, having been verified by hundreds of subsequent studies seeking to replicate and extend the pioneering work of Li *et al.* (reviewed in Fan *et al.*[25] and Subramaniam *et al.*[26]). However, the demonstrable absence of RUNX3 from normal GECs, the progenitors to GC, casts doubt upon its much vaunted TSG function.[27] By inference, the existing model of P2 hypermethylation as a driver of GC is also inadequate given that *RUNX3* is repressed by default in normal GECs and is often overexpressed in GC and other cancers.

We propose an alternative model in which differential methylation of P1 dictates lineage-specific *RUNX3* expression. This novel modality was evident from observations in normal GEC and mesenchymal (fibroblast) lineages, where P1 was hypermethylated and repressed. By contrast, in immune lineages P1 lacked methylation and was widely transcribed. The fact that not all immune cell types have Runx3 expression, despite their universal P1

hypomethylation, argues that *trans*-factors are also required for full activation of transcription. This mode of differential methylation was highly significant in the context of human and mouse GC progression. P1 hypomethylation (and increased transcription) signatures reflected evolving cell-type composition of the preneoplastic epithelium and/or tumour microenvironment due to immune cell recruitment. Moreover, localization of RUNX3 to immune cells infiltrating the preneoplastic and tumour epithelium as shown here excludes the possibility that preneoplastic epithelial lesions, such as atrophic gastritis or mucous cell metaplasia, may have influenced P1 transcription and/or methylation. In breast cancer, DNA methylation profiles reflecting the tumour immune component have been used to great effect for clinical prediction.[14] Presence of T-cell 'methylation biomarkers' in breast tumours correlated with better prognosis, suggesting a link with anti-tumour immunity. We postulate that *RUNX3* P1 hypomethylation, as a marker of cytotoxic lymphocytes, may have similar prognostic value in GC, a postulate supported by the fact that cytolytic properties of CD8+ T-cells and NK cells are *Runx3*-dependent.[23]

A second major conclusion here is that P2 hypermethylation is a phenotypic feature of transformed, or immortal, GECs and has no causal role in *RUNX3* repression or GC pathogenesis. Our findings are reminiscent of recent work in hTERT-immortalized fibroblasts showing progressive accumulation of P2 hypermethylation as a function of increasing generations in culture, without affecting transcription.[40] However, our findings make the key distinction of showing evolution of immortal P2 hypermethylated clones from primary GECs ostensibly lacking P2 methylation. Whether P2 hypermethylation can arise *de novo* in culture, or amplifies clonally from rare aberrant cells in primary tumours, remains to be elucidated. Resonant with our findings, repressed CGI promoters are more vulnerable to de novo methylation in cancer than active CGI promoters[10,38] based on polycomb-mediated premarking by repressive histone (H)3-lysine (K)27 tri-methylation.[41] Together with evidence that the polycomb repressor complex 2 can promote *RUNX3* P2 repression in GEC,[42] these studies illustrate how a program of DNA methylation-independent repression might promote *de novo* P2 hypermethylation in immortal GECs. Nonetheless, it is increasingly apparent that CGI hypermethylation is less frequent in cancer than initially hypothesized.[43] We indeed observed lower P2 methylation frequencies here using quantitative EpiTYPER analysis than reported by earlier studies using nonquantitative methylation-specific PCR (MSP).[25,26] The propensity of non-quantitative MSP to overestimate low methylation levels[44] may explain this discrepancy. In agreement, recent work found that P2 methylation levels of <10% can be reported as 'hypermethylated' by MSP.[45]

With its TSG function now in doubt,[27] alternative roles for *RUNX3* in the stomach must be considered. It has not escaped our notice that gastric epithelial hyperplasia in *Runx3*$^{-/-}$ mice may arise by a non-autonomous mechanism. This phenotype was attributed to *Runx3* deficiency in CD8+ cytolytic T-cells and consequent impairment of anti-tumour immunity.[46] An immune-specific anti-tumour role was similarly implicated by spontaneous colitis and tumour growth in mice with lymphocyte-specific *Runx3* deficiency.[47] It may be significant that *Runx3* expression is particularly abundant in immune lineages with known roles in anti-tumour immunity. *Runx3* is essential for the cytolytic functions of CD8+ T-cells

and NK cells,[19,23] but if either of these modalities might extend to restrain gastric tumour growth remains to be proven.

Here we have proposed a new model of *RUNX3* epigenetic control based on lineage-specific hypomethylation of its (non-CGI) P1 promoter in immune cells. Furthermore, aberrant *RUNX3* P1 hypomethylation derives from the mobile immune component of the preneoplastic and tumour epithelium during GC development. The significance of this new data lies in the potential clinical utility of P1 methylation in identifying 'at-risk' individuals during the preneoplastic stages of GC, before the emergence of malignant adenocarcinoma. P1 methylation may therefore offer superior clinical potential to P2 methylation, which appears later in GC progression and, reportedly, has no predictive value in staging, prognosis, recurrence or survival.[25]

MATERIALS AND METHODS

Human tissues

H. pylori-infected and uninfected human gastric epithelial tissues, GCs and preneoplastic adjacent to cancer tissues with IM were obtained endoscopically as described.[6] Ethics approvals were obtained from the Royal Melbourne Hospital Human Research Ethics Committee (approval number 2004.176) and the Kanazawa University Ethics Committee for Human Genome Research (approval number 174.2008). Written informed consent was obtained for all study participants.

Mice

H+/K+ATPase-gmcsf transgenic mice[36] were maintained on a Balb/C genetic background. *Gp130*$^{F/F}$ co-receptor knock-in mice[37] were maintained on a C57BL6/J genetic background. WT littermate controls were used in all the experiments. Mice were housed under specific pathogenfree conditions. Experiments were approved by the Murdoch Children's Research Institute Animal Ethics Committee (approval numbers A693 and A713). WT (C57BL6) mice were infected with the *H. pylori* Sydney strain (SS) 1 as described.[6]

Mammalian cell culture

Human GC cell lines AGS, MKN7, MKN28, NCI-SNU1, KATO III and NCI-N87 were cultured in RPMI 1640 Glutamax medium supplemented with 10% fetal bovine serum (FBS); 2 mM non-essential amino acids; 50 IU penicillin; 50ug/ml streptomycin (Invitrogen, Carlsbad, CA, USA) at 37 °C in a humidified incubator with 5% CO_2/air. To derive mouse primary GECs, stomachs from 3-week-old mice were chopped into ~1-mm^3 pieces and digested with 2 mg/ml collagenase A (Roche, Mannheim, Germany) at 37 °C for 1 h. Digested tissue was resuspended in Dulbecco's modified Eagle's medium Glutamax medium supplemented with 20% FBS, 2 mM non-essential amino acids; 50IU penicillin; 50ug/ml streptomycin (Invitrogen), disaggregated by repeated pipetting, seeded into 24-well plates and incubated at 37 °C with 5% CO_2/air for 48 h to allow for culture maturation. To derive immortal mouse GEC lines, freshly dissected *gp130*$^{F/F}$ gastric tumours were surface sterilized by incubation in 0.04% sodium hypochlorite in phosphate-buffered saline (PBS)

for 20 min at room temperature, rinsed in PBS, chopped into ~1-mm^3 pieces, resuspended in sterile PBS and allowed to settle for 1 min. Supernatants were aspirated, and tissue was collected by centrifugation, resuspended in 1 mg/ml collagenase and 1 IU/ml neutral protease (Sigma, St Louis, MO, USA) in PBS and digested at 37 °C for 60 min. Digested tissue was collected by centrifugation, resuspended in growth medium[48] seeded onto collagen-coated 24-well culture plates and incubated undisturbed for 7 days. Rapidly expanding epithelial clones were isolated from contaminating non-epithelial cells by limiting dilution.

Generation of bone marrow-derived cultured MCs

Bone marrow stem cells were extracted from femurs of 6–8-week-old C57BL6 mice and cultured in Dulbecco's modified Eagle's medium Glutamax medium, supplemented with 10% FBS, 50 IU penicillin, 50 ug/ml streptomycin and IL-3 for 6 weeks as described.[49] IL-3-enriched medium was sourced from murine WEHI-3 myelomonocytic leukaemia cultures and added to growth medium at 20%v/v.[50] MC differentiation was verified by cell surface staining with CD117-FITC (fluorescein isothiocyanate; 1:300) and FcεR1α-PE (1:300; BD Biosciences, San Jose, CA, USA). Stained cells were analysed on a LSR-II flow cytometer using the FacsDiva software (BD Biosciences).

Immunohistochemistry and immunofluorescence

Immunohistochemistry with peroxidase detection was done essentially as described.[51] A well-characterized rabbit polyclonal anti-Runx3 antiserum (poly-G) was used at a dilution of 1:1000.[52] Bound immunocomplexes were detected using Vectastain ABC reagents (Vector Laboratories, Burlingame, CA, USA), and staining was visualized by incubation in 3, 3′-diaminobenzidine tetrahydrochloride buffer (Sigma). Immunofluorescence in cultured cells was performed as described.[51] A FITC-conjugated rat polyclonal anti-mouse cytokeratin (Krt)8 antibody (Sigma) was used at a dilution of 1:100.

FACS

Splenocytes were prepared from 12-week mice, erythrocytes were removed by incubation in lysis buffer (1:9 v/v 0.17M Tris: 0.16 M ammonium chloride) for 5 min and enriched splenocytes were resuspended in 2% FBS and 1 mM EDTA in Hank's Balanced Salt Solution. For isolation of tumour lineages, dissected *gp130*$^{F/F}$ gastric tumours were chopped into ~3–4mm^3 pieces and disaggregated non-enzymatically by incubation in dissociation buffer (5% FBS, 1 mM dithiothreitol, 1 mM EDTA in PBS) for 1 h at 37 °C with agitation. Digested tissue pieces were passed through a 70-μm strainer, and the cells were resuspended in 2% FBS and 2 mM EDTA in Hank's Balanced Salt Solution. Splenocytes and gastric tumour cells were stained with CD11c-APC (1:500), CD8α-APC-Cy7 (1:500), CD45R/B221-FITC (1:500), CD11b-PE (1:500), Gr-1 (Ly6-G/C)-PerCP-Cy5.5 (1:300) (all from BD Biosciences) and NK1.1-brilliant violet 421 (1:300) E-cadherin-PE (1:300) (from BioLegend, San Diego, CA, USA). Cells were sorted (at low pressure with a 100-μm nozzle) on a MoFlo sorter (Beckman-Coulter, Brea, CA, USA). Cells were not cultured in the period between isolation and sorting.

Gene expression and DNA methylation analysis

QRT–PCR was performed as described.[53] Primer sequences (Supplementary Table S2) were designed using the primer3 tool (http://frodo.wi.mit.edu/primer3/). Relative gene expression was normalized to the reference genes *GAPDH* (glyceraldehyde 3-phosphate dehydrogenase; human) or *Rpl32* (mouse) using $-2\Delta\Delta Ct = \Delta Ct$ sample$-\Delta Ct$ calibrator. Quantitative DNA methylation analysis was performed by EpiTYPER (Sequenom, San Diego, CA, USA) as described.[6] Primer sequences for methylation amplicons (Supplementary Table S3) were selected using EpiDesigner (http://www.epidesigner.com). Data cleaning and hierarchical clustering were performed in R script using the gplots package (http://www.r-project.org/).

Statistical analysis

Data were analysed with GraphPad Prism V5.1 software (GraphPad Software, La Jolla, CA, USA). Data were expressed as mean ± s.e.m. Statistical analysis was performed by one-way analysis of variance and the appropriate parametric or nonparametric post test. *P*-values of ≤ 0.05 were considered statistically significant.

Supplementary Material

Refer to Web version on PubMed Central for supplementary material.

Acknowledgments

We thank Professor Y Groner and Dr D Levanon (The Weizmann Institute of Science, Rehovot, Israel) for their gift of anti-Runx3 antiserum and critical reviews of the manuscript. We thank Professor I van Driel (University of Melbourne, Australia) for providing *H*+/*K*+ ATPase-gmcsf transgenic mice and Professor M Ernst (Walter and Eliza Hall Institute of Medical Research, Melbourne, Australia) for providing *gp130*$^{F/F}$ mice. We thank Dr J Däbritz (Murdoch Children's Research Institute) for critically reviewing the manuscript. This work was supported by a project grant (1006542) awarded to TRM by the National Health and Medical Research Council (NH&MRC) of Australia and by the Victorian Government's Medical Research Operational Infrastructure Program.

ABBREVIATIONS

CGI	CpG island
CpG	cytidine-phosphate-guanidine
DC	dendritic cell
GC	gastric cancer
GEC	gastric epithelial cell
hTERT	human telomerase reverse transcriptase
IM	intestinal metaplasia
MC	mast cell
MSP	methylation-specific PCR
NK	natural killer
RUNX	runt-domain family transcription factor

TSG tumour-suppressor gene

References

1. Ferlay, J.; Soerjomataram, I.; Ervik, M.; Dikshit, R.; Eser, S.; Mathers, C., et al. GLOBOCAN 2012 v1.0, Cancer Incidence and Mortality Worldwide: IARC CancerBase No. 11 [Internet]. International Agency for Research on Cancer; Lyon, France: 2013.
2. Yeoh KG. How do we improve outcomes for gastric cancer? J Gastroenterol Hepatol. 2007; 22:970–972. [PubMed: 17524038]
3. Correa P, Haenszel W, Cuello C, Tannenbaum S, Archer M. A model for gastric cancer epidemiology. Lancet. 1975; 2:58–60. [PubMed: 49653]
4. Schier S, Wright NA. Stem cell relationships and the origin of gastrointestinal cancer. Oncology. 2005; 69(Suppl 1):9–13. [PubMed: 16210870]
5. Hoffmann W. Self-renewal of the gastric epithelium from stem and progenitor cells. Front Biosci (Schol Ed). 2013; 5:720–731. [PubMed: 23277081]
6. Peterson AJ, Menheniott TR, O'Connor L, Walduck AK, Fox JG, Kawakami K, et al. *Helicobacter pylori* infection promotes methylation and silencing of trefoil factor 2, leading to gastric tumor development in mice and humans. Gastroenterology. 2010; 139:2005–2017. [PubMed: 20801119]
7. Schmid CA, Muller A. FoxD3 is a novel, epigenetically regulated tumor suppressor in gastric carcinogenesis. Gastroenterology. 2013; 144:22–25. [PubMed: 23164571]
8. Ehrlich M. DNA methylation in cancer: too much, but also too little. Oncogene. 2002; 21:5400–5413. [PubMed: 12154403]
9. Clark SJ, Melki J. DNA methylation and gene silencing in cancer: which is the guilty party? Oncogene. 2002; 21:5380–5387. [PubMed: 12154400]
10. Sproul D, Nestor C, Culley J, Dickson JH, Dixon JM, Harrison DJ, et al. Transcriptionally repressed genes become aberrantly methylated and distinguish tumors of different lineages in breast cancer. Proc Natl Acad Sci USA. 2011; 108:4364–4369. [PubMed: 21368160]
11. Dedeurwaerder S, Fuks F. DNA methylation markers for breast cancer prognosis: unmasking the immune component. Oncoimmunology. 2012; 1:962–964. [PubMed: 23162772]
12. Weber M, Hellmann I, Stadler MB, Ramos L, Paabo S, Rebhan M, et al. Distribution, silencing potential and evolutionary impact of promoter DNA methylation in the human genome. Nat Genet. 2007; 39:457–466. [PubMed: 17334365]
13. Schmidl C, Klug M, Boeld TJ, Andreesen R, Hoffmann P, Edinger M, et al. Lineage-specific DNA methylation in T cells correlates with histone methylation and enhancer activity. Genome Res. 2009; 19:1165–1174. [PubMed: 19494038]
14. Dedeurwaerder S, Desmedt C, Calonne E, Singhal SK, Haibe-Kains B, Defrance M, et al. DNA methylation profiling reveals a predominant immune component in breast cancers. EMBO Mol Med. 2011; 3:726–741. [PubMed: 21910250]
15. Hu M, Yao J, Cai L, Bachman KE, van den Brule F, Velculescu V, et al. Distinct epigenetic changes in the stromal cells of breast cancers. Nat Genet. 2005; 37:899–905. [PubMed: 16007089]
16. Westendorf JJ, Hiebert SW. Mammalian runt-domain proteins and their roles in hematopoiesis, osteogenesis, and leukemia. J Cell Biochem. 1999; (Suppl 32–33):51–58. [PubMed: 10629103]
17. Lian JB, Javed A, Zaidi SK, Lengner C, Montecino M, van Wijnen AJ, et al. Regulatory controls for osteoblast growth and differentiation: role of Runx/Cbfa/AML factors. Crit Rev Eukaryot Gene Expr. 2004; 14:1–41. [PubMed: 15104525]
18. Levanon D, Bettoun D, Harris-Cerruti C, Woolf E, Negreanu V, Eilam R, et al. The Runx3 transcription factor regulates development and survival of TrkC dorsal root ganglia neurons. EMBO J. 2002; 21:3454–3463. [PubMed: 12093746]
19. Woolf E, Xiao C, Fainaru O, Lotem J, Rosen D, Negreanu V, et al. Runx3 and Runx1 are required for CD8 T cell development during thymopoiesis. Proc Natl Acad Sci USA. 2003; 100:7731–7736. [PubMed: 12796513]

20. Taniuchi I, Osato M, Egawa T, Sunshine MJ, Bae SC, Komori T, et al. Differential requirements for Runx proteins in CD4 repression and epigenetic silencing during T lymphocyte development. Cell. 2002; 111:621–633. [PubMed: 12464175]
21. Fainaru O, Woolf E, Lotem J, Yarmus M, Brenner O, Goldenberg D, et al. Runx3 regulates mouse TGF-beta-mediated dendritic cell function and its absence results in airway inflammation. EMBO J. 2004; 23:969–979. [PubMed: 14765120]
22. Lai CB, Mager DL. Role of runt-related transcription factor 3 (RUNX3) in transcription regulation of natural cytotoxicity receptor 1 (NCR1/NKp46), an activating natural killer (NK) cell receptor. J Biol Chem. 2012; 287:7324–7334. [PubMed: 22253448]
23. Levanon D, Negreanu V, Lotem J, Bone KR, Brenner O, Leshkowitz D, et al. Runx3 regulates interleukin-15 dependent natural killer cell activation. Mol Cell Biol. 2014; 34:1158–1169. [PubMed: 24421391]
24. Li QL, Ito K, Sakakura C, Fukamachi H, Inoue K, Chi XZ, et al. Causal relationship between the loss of RUNX3 expression and gastric cancer. Cell. 2002; 109:113–124. [PubMed: 11955451]
25. Fan XY, Hu XL, Han TM, Wang NN, Zhu YM, Hu W, et al. Association between RUNX3 promoter methylation and gastric cancer: a meta-analysis. BMC Gastro-enterol. 2011; 11:92.
26. Subramaniam MM, Chan JY, Yeoh KG, Quek T, Ito K, Salto-Tellez M. Molecular pathology of RUNX3 in human carcinogenesis. Biochim Biophys Acta. 2009; 1796:315–331. [PubMed: 19682550]
27. Levanon D, Bernstein Y, Negreanu V, Bone KR, Pozner A, Eilam R, et al. Absence of Runx3 expression in normal gastrointestinal epithelium calls into question its tumour suppressor function. EMBO Mol Med. 2011; 3:593–604. [PubMed: 21786422]
28. Salto-Tellez M, Peh BK, Ito K, Tan SH, Chong PY, Han HC, et al. RUNX3 protein is overexpressed in human basal cell carcinomas. Oncogene. 2006; 25:7646–7649. [PubMed: 16767156]
29. Li J, Kleeff J, Guweidhi A, Esposito I, Berberat PO, Giese T, et al. RUNX3 expression in primary and metastatic pancreatic cancer. J Clin Pathol. 2004; 57:294–299. [PubMed: 14990603]
30. Kudo Y, Tsunematsu T, Takata T. Oncogenic role of RUNX3 in head and neck cancer. J Cell Biochem. 2011; 112:387–393. [PubMed: 21268058]
31. Hu SL, Huang DB, Sun YB, Wu L, Xu WP, Yin S, et al. Pathobiologic implications of methylation and expression status of Runx3 and CHFR genes in gastric cancer. Med Oncol. 2011; 28:447–454. [PubMed: 20300977]
32. Gardiner-Garden M, Frommer M. CpG islands in vertebrate genomes. J Mol Biol. 1987; 196:261–282. [PubMed: 3656447]
33. Han H, Cortez CC, Yang X, Nichols PW, Jones PA, Liang G. DNA methylation directly silences genes with non-CpG island promoters and establishes a nucleosome occupied promoter. Hum Mol Genet. 2011; 20:4299–4310. [PubMed: 21835883]
34. Jackson CB, Judd LM, Menheniott TR, Kronborg I, Dow C, Yeomans ND, et al. Augmented gp130-mediated cytokine signalling accompanies human gastric cancer progression. J Pathol. 2007; 213:140–151. [PubMed: 17724739]
35. Coolen MW, Statham AL, Gardiner-Garden M, Clark SJ. Genomic profiling of CpG methylation and allelic specificity using quantitative high-throughput mass spectrometry: critical evaluation and improvements. Nucleic Acids Res. 2007; 35:e119. [PubMed: 17855397]
36. Biondo M, Nasa Z, Marshall A, Toh BH, Alderuccio F. Local transgenic expression of granulocyte macrophage-colony stimulating factor initiates autoimmunity. J Immunol. 2001; 166:2090–2099. [PubMed: 11160260]
37. Judd LM, Alderman BM, Howlett M, Shulkes A, Dow C, Moverley J, et al. Gastric cancer development in mice lacking the SHP2 binding site on the IL-6 family co-receptor gp130. Gastroenterology. 2004; 126:196–207. [PubMed: 14699500]
38. Keshet I, Schlesinger Y, Farkash S, Rand E, Hecht M, Segal E, et al. Evidence for an instructive mechanism of de novo methylation in cancer cells. Nat Genet. 2006; 38:149–153. [PubMed: 16444255]

39. Smiraglia DJ, Rush LJ, Fruhwald MC, Dai Z, Held WA, Costello JF, et al. Excessive CpG island hypermethylation in cancer cell lines versus primary human malignancies. Hum Mol Genet. 2001; 10:1413–1419. [PubMed: 11440994]
40. Landan G, Cohen NM, Mukamel Z, Bar A, Molchadsky A, Brosh R, et al. Epigenetic polymorphism and the stochastic formation of differentially methylated regions in normal and cancerous tissues. Nat Genet. 2012; 44:1207–1214. [PubMed: 23064413]
41. Schlesinger Y, Straussman R, Keshet I, Farkash S, Hecht M, Zimmerman J, et al. Polycomb-mediated methylation on Lys27 of histone H3 pre-marks genes for de novo methylation in cancer. Nat Genet. 2007; 39:232–236. [PubMed: 17200670]
42. Fujii S, Ito K, Ito Y, Ochiai A. Enhancer of zeste homologue 2 (EZH2) down-regulates RUNX3 by increasing histone H3 methylation. J Biol Chem. 2008; 283:17324–17332. [PubMed: 18430739]
43. Weber M, Davies JJ, Wittig D, Oakeley EJ, Haase M, Lam WL, et al. Chromosome-wide and promoter-specific analyses identify sites of differential DNA methylation in normal and transformed human cells. Nat Genet. 2005; 37:853–862. [PubMed: 16007088]
44. Esteller M, Corn PG, Baylin SB, Herman JG. A gene hypermethylation profile of human cancer. Cancer Res. 2001; 61:3225–3229. [PubMed: 11309270]
45. So K, Tamura G, Honda T, Homma N, Endoh M, Togawa N, et al. Quantitative assessment of RUNX3 methylation in neoplastic and non-neoplastic gastric epithelia using a DNA microarray. Pathol Int. 2006; 56:571–575. [PubMed: 16984612]
46. Brenner O, Levanon D, Negreanu V, Golubkov O, Fainaru O, Woolf E, et al. Loss of Runx3 function in leukocytes is associated with spontaneously developed colitis and gastric mucosal hyperplasia. Proc Natl Acad Sci USA. 2004; 101:16016–16021. [PubMed: 15514019]
47. Sugai M, Aoki K, Osato M, Nambu Y, Ito K, Taketo MM, et al. Runx3 is required for full activation of regulatory T cells to prevent colitis-associated tumor formation. J Immunol. 2011; 186:6515–6520. [PubMed: 21515792]
48. Whitehead, RH. Establishment of cell lines from colon carcinoma. In: Freshney, IR., editor. Culture of Human Tumor Cells. John Wiley and Sons; New York, NY, USA: 2003. p. 68-80.
49. Huber M, Helgason CD, Damen JE, Liu L, Humphries RK, Krystal G. The src homology 2-containing inositol phosphatase (SHIP) is the gatekeeper of mast cell degranulation. Proc Natl Acad Sci USA. 1998; 95:11330–11335. [PubMed: 9736736]
50. Kalesnikoff J, Galli SJ. Antiinflammatory and immunosuppressive functions of mast cells. Methods Mol Biol. 2011; 677:207–220. [PubMed: 20941613]
51. Menheniott TR, Peterson AJ, O'Connor L, Lee KS, Kalantzis A, Kondova I, et al. A novel gastrokine, Gkn3, marks gastric atrophy and shows evidence of adaptive gene loss in humans. Gastroenterology. 2010; 138:1823–1835. [PubMed: 20138039]
52. Levanon D, Brenner O, Negreanu V, Bettoun D, Woolf E, Eilam R, et al. Spatial and temporal expression pattern of Runx3 (Aml2) and Runx1 (Aml1) indicates non-redundant functions during mouse embryogenesis. Mech Dev. 2001; 109:413–417. [PubMed: 11731260]
53. Lee KS, Kalantzis A, Jackson CB, O'Connor L, Murata-Kamiya N, Hatakeyama M, et al. *Helicobacter pylori* CagA triggers expression of the bactericidal lectin REG3gamma via gastric STAT3 activation. PLoS ONE. 2012; 7:e30786. [PubMed: 22312430]

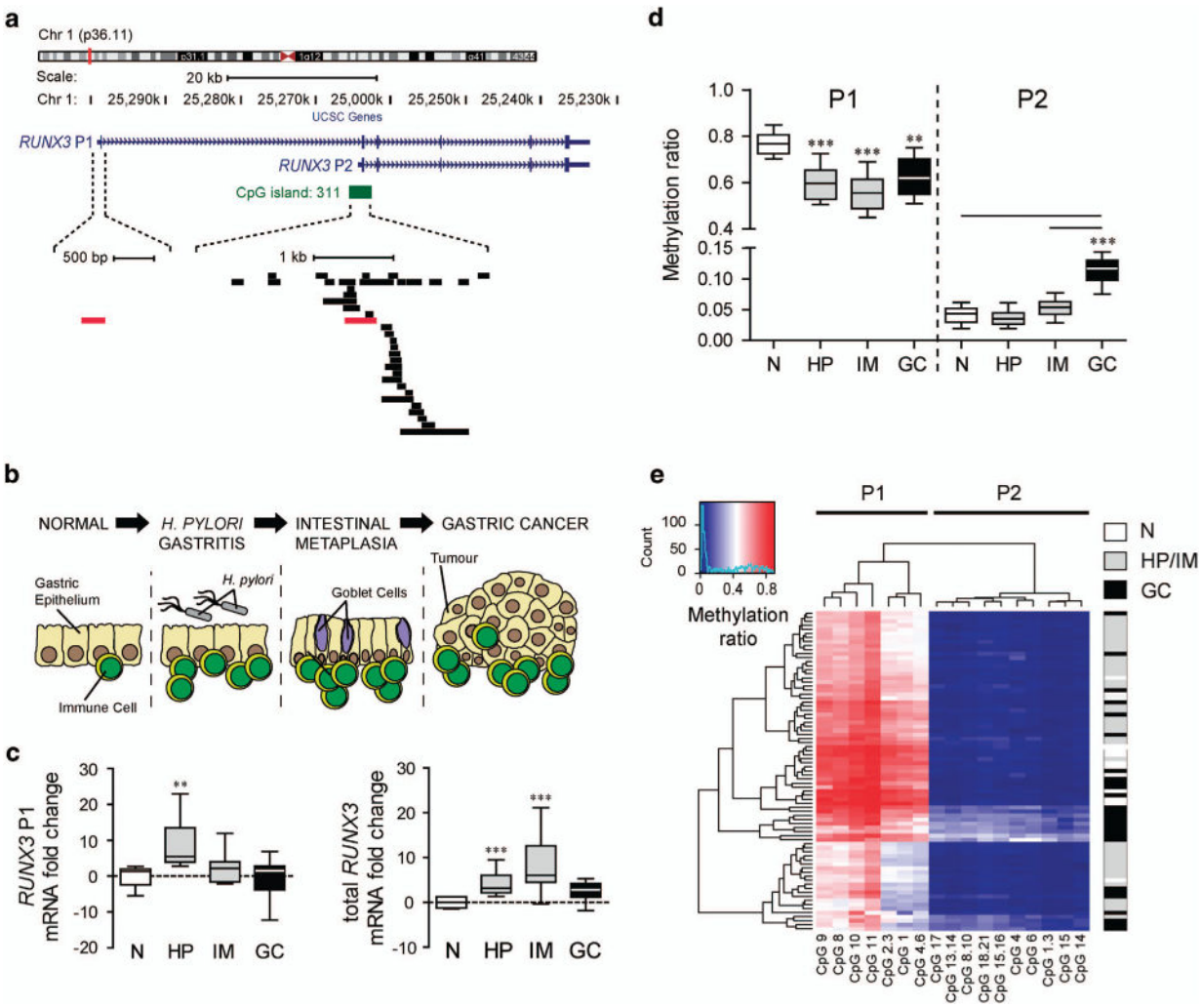

Figure 1.

Epigenetic regulation of *RUNX3* P1 in human GC. (**a**) Mapping of methylation amplicons within human RUNX3. Genome browser output for human *RUNX3* on chromosome 1p36 (GRCh37 Hg19; http://genome.ucsc.edu/) shows relative locations of P1 and P2 promoter regions and intron/exon structures of the derived transcripts. Browser tracks show locations of *RUNX3* methylation amplicons (from previously published studies, black bars; from current study, red bars) aligned with the human genome using the 'Blast Like Alignment Tool' (BLAT). (**b**) Schematic showing progressive alteration in cell-type composition of the gastric epithelium during human GC progression. (**c**) QRT–PCR analysis of *RUNX3* mRNA expression in human GC progression. Box plots show mRNA fold change relative to GAPDH (glyceraldehyde 3-phosphate dehydrogenase) internal reference gene expression for normal (N; *n*=6), *H. pylori*-infected (HP; *n* = 16), preneoplastic adjacent to tumour with intestinal metaplasia (IM; *n=28)* and gastric cancer (GC; *n=28*) mucosal tissues. (**d**) EpiTYPER analysis of *RUNX3* P1 and P2 methylation in tissue samples analysed in panel (**b**). Box plots show combined CpG methylation values for P1 and P2, respectively. (e) Heatmap showing two-way hierarchical clustering of methylation data presented in panel (**c**). CpGs are shown on the horizontal axis; tissue samples are shown on the vertical axis.

Tissue identities are indicated to the right of the heatmap. Asterisks show statistical significance: $^{**}P < 0.01$; $^{***}P < 0.001$.

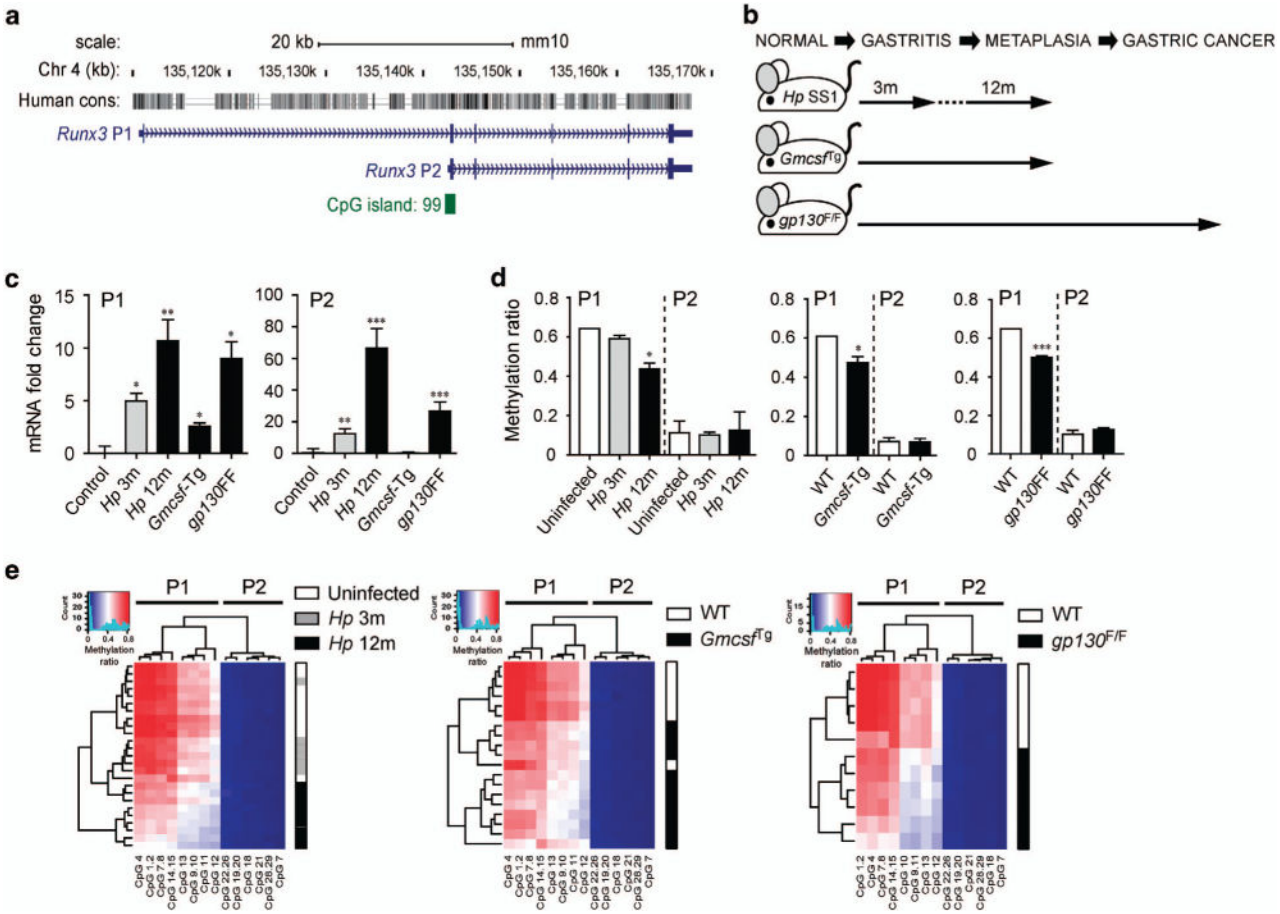

Figure 2.

Conserved *Runx3* P1 hypomethylation in mouse gastric inflammation and tumorigenesis. (**a**) Genome browser output for the mouse Runx3 locus on chromosome 4qD3 (GRCm38/mm10; http://genome.ucsc.edu/) shows relative locations of P1 and P2 promoters and intron/exon structure of their transcripts. (**b**) Schematic showing the mouse genetic and infection models used to recapitulate key stages of human GC progression. (**c**) QRT–PCR analysis of *Runx3* P1 and P2 transcripts in stomach tissues collected from C57BL6 (WT) mice infected with *H. pylori* SS1 for 3 months (*Hp* 3m) and 12 months (*Hp* 12m) in $Gmcsf^{Tg}$ and $gp130^{F/F}$ mice. Histograms show mRNA fold change relative to uninfected or WT controls. (**d**) EpiTYPER quantitative DNA methylation analysis of *Runx3* P1 and P2 promoters of gastric tissues analysed for mRNA in panel (**b**). Histograms show the combined CpG methylation levels for P1 and P2, respectively. Error bars ± s.e.m. Asterisks show statistical significance: $*P < 0.05$; $**P < 0.01$; $***P<0.001$. (**e**) Heatmaps show two-way hierarchical clustering of P1 and P2 individual CpG methylation values for data shown in panel (**d**).

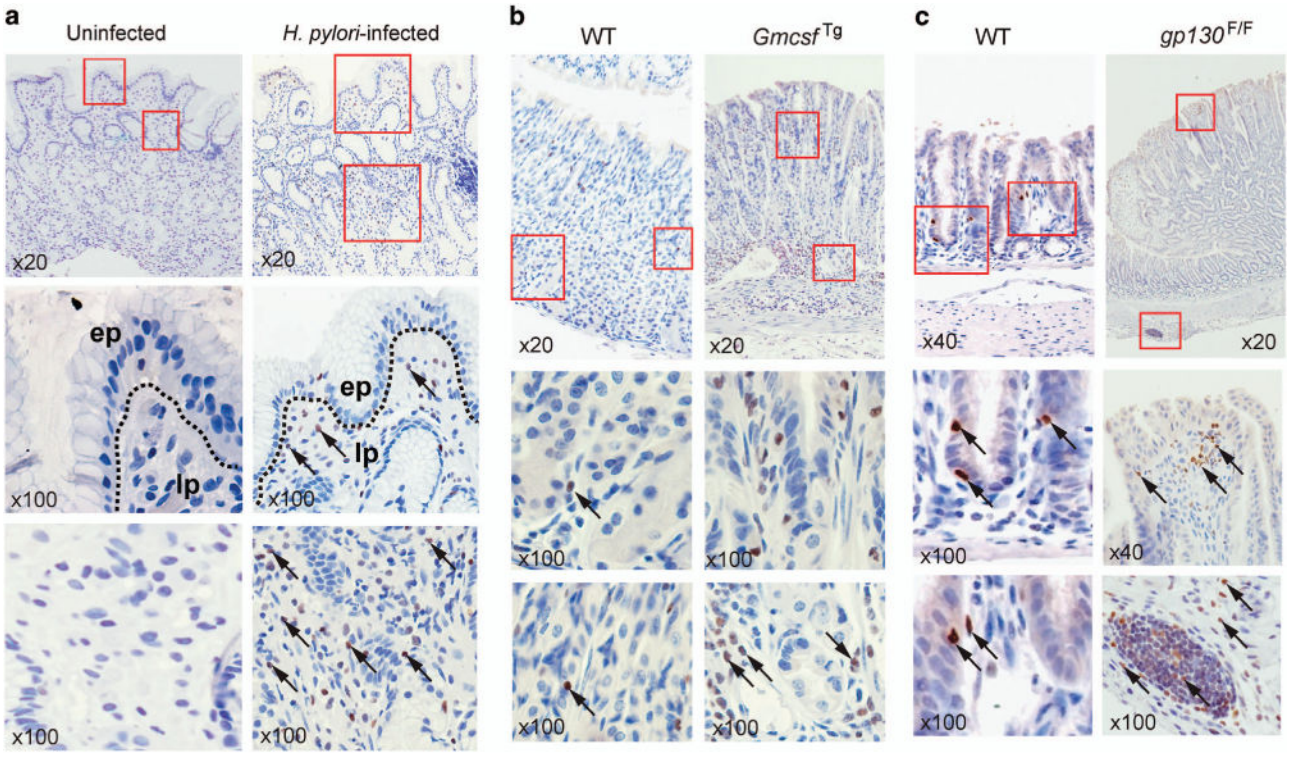

Figure 3.

Immunolocalization of RUNX3 in human and murine gastric preneoplasia and tumorigenesis. (**a**) RUNX3 immunohistochemistry in human gastric mucosal tissue collected from *H. pylori*-infected and uninfected individuals. (**b**) Runx3 immunohistochemistry in *Gmcsf*^{Tg} gastric fundus. (**c**) Runx3 immunohistochemistry in *gp130*$^{F/F}$ gastric antral tumours. Tissue sections were counterstained with hematoxylin (blue staining). Magnifications are indicated (×20, ×40, ×100). Arrows indicate highly discrete Runx3 nuclear staining. lp, lamina propria; ep, epithelium.

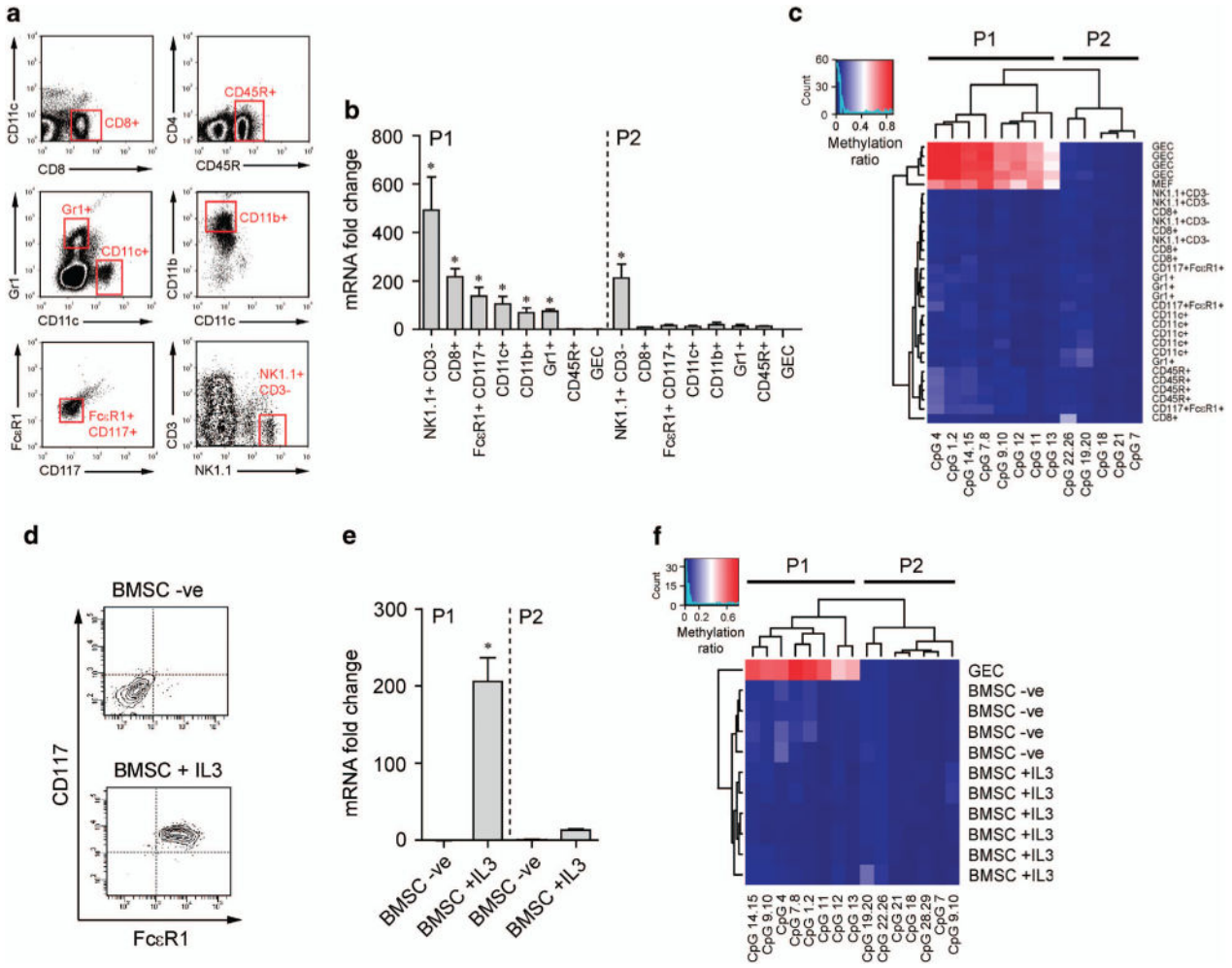

Figure 4.

Differential *Runx3* P1 methylation in GEC and hematopoietic lineages. (**a**) Isolation of immune cell populations from splenocytes by FACS: NK1.1+ CD3− NK cells; CD3+CD8+ T-cells; CD117+ FcεR1a+ MCs; CD11c+ DCs; CD11b+ macrophages; Gr1+ neutrophils; and CD45R+ B-cells. (**b**) QRT–PCR analysis of *Runx3* P1 and P2 transcripts in FACS-sorted immune cell types. Histograms show mRNA fold changes relative to levels in primary GEC. (**c**) Quantitative DNA methylation analysis of Runx3 P1 and P2 promoters in FACS-sorted immune cell types, primary GECs and primary mouse embryonic fibroblasts. Heatmap showing two-way hierarchical clustering of P1 and P2 methylation data. (**d**) *In vitro* generation of bone marrow-derived MCs. Flow cytometric analysis of murine bone marrow stem cells (BMSC) cultured with IL-3 (BMSC+IL3) or untreated (BMSC –ve). MC differentiation is shown by the acquisition of a CD117+ FcεR1+ double-positive phenotype (one representative experiment of four replicates is shown). (**e**) QRT–PCR analysis of *Runx3* P1 and P2 mRNA in BMSC+IL3 and BMSC control cultures. Error bars ± s.e.m. Asterisks show statistical significance: $*P < 0.05$. (**f**) Heatmap showing EpiTYPER quantitative methylation analysis of Runx3 P1 and P2 promoters corresponding to the samples analysed in panel (**e**).

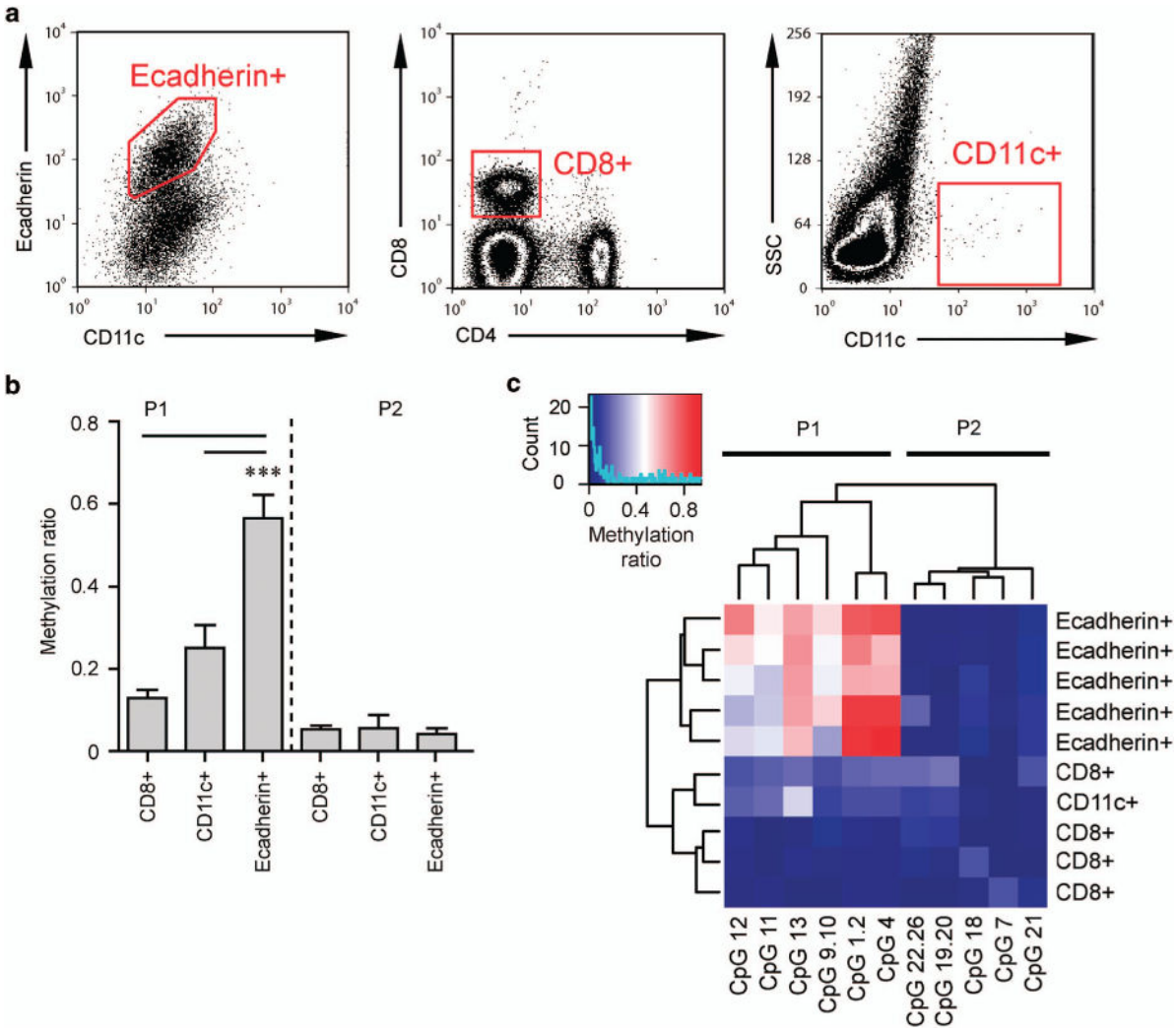

Figure 5.

Runx3 P1 methylation in gastric tumour lineages. (**a**) Isolation of immune cells and GECs from *gp130*$^{F/F}$ gastric tumour tissue by FACS: CD8+ T-cells; CD11c+ DCs; and e-cadherin + GECs. Shown is one representative example of five replicate experiments. (**b**) EpiTYPER quantitative DNA methylation analysis of *Runx3* P1 and P2 promoters of isolated cell types shown in panel (**a**). Histograms show the combined CpG methylation levels for P1 and P2, respectively. Error bars ± s.e.m. Asterisks show statistical significance: ***$P < 0.001$. (**c**) Heatmap showing two-way hierarchical clustering of P1 and P2 individual CpG methylation data represented in panel (**b**).

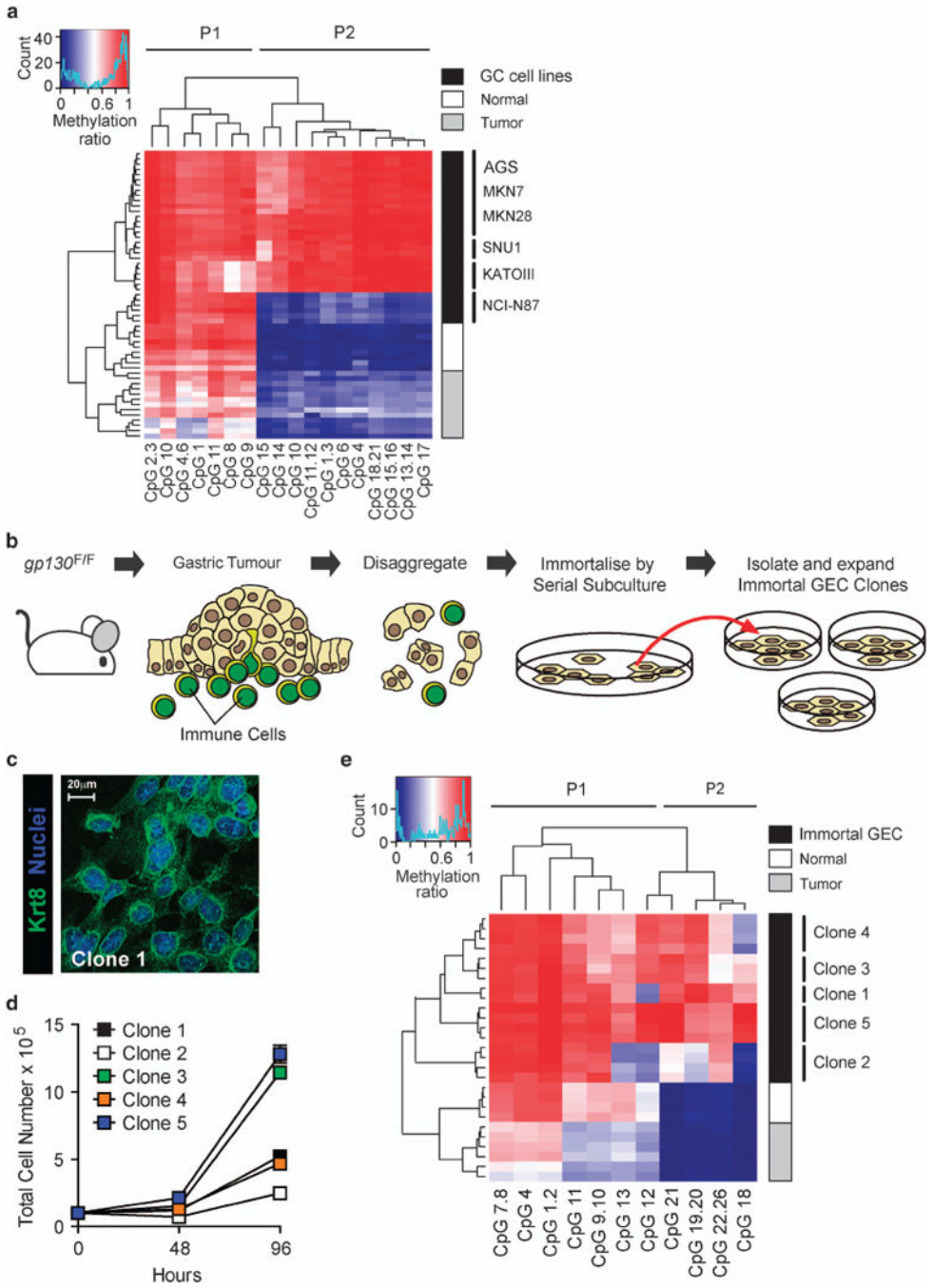

Figure 6.

RUNX3 P2 methylation is triggered by immortalization of human and mouse GECs. (**a**) EpiTYPER analysis of *RUNX3* P2 (and P1) methylation levels in human GC cell lines, primary GC tumours and normal gastric epithelial tissues. Heatmap shows two-way hierarchical clustering of individual CpG methylation values against cell line or tissue type. (**b**) Flow diagram showing the derivation of mouse immortal GEC lines from *gp130*$^{F/F}$ primary gastric epithelial tumours. (**c**) Immunofluorescent detection of cytokeratin (Krt)8 in immortal GEC lines. Representative staining for one of the lines (clone 1) is shown. (**d**)

Growth curves of mouse immortal GEC lines in monolayer culture. Viable cell count data are shown as the mean of six replicate wells for each clone. (**e**) EpiTYPER analysis of *Runx3* P1 and P2 methylation in immortal mouse GEC, primary *gp130*$^{F/F}$ tumours and WT gastric tissue. Heatmaps show two-way hierarchical clustering of individual CpG methylation values for P1 and P2.

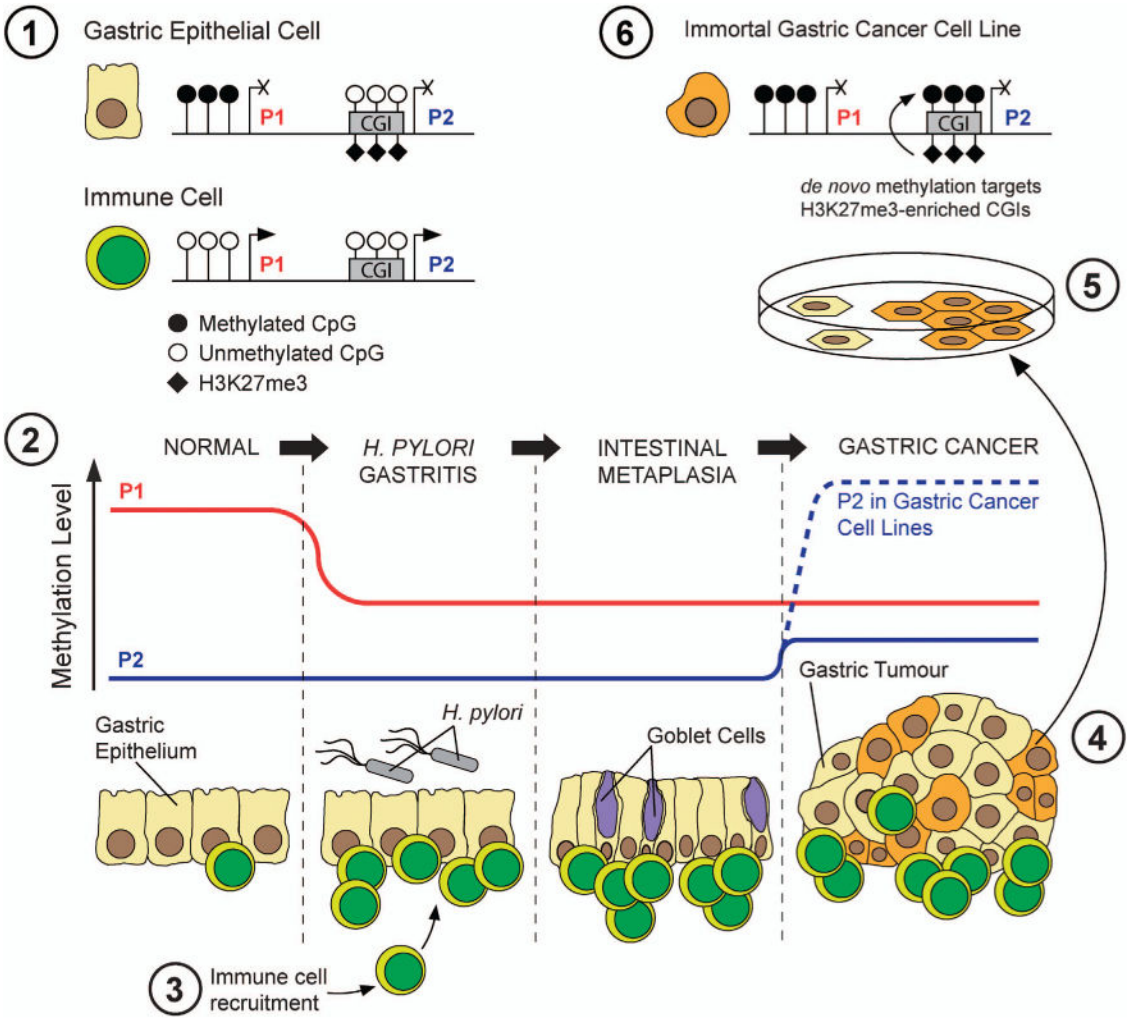

Figure 7.

Schematic showing effects of cell-type composition and tumour clonality on *RUNX3* promoter methylation in GC progression and cell line establishment. In GECs, P1 is hypermethylated and repressed. In immune cells, P1 is hypomethylated and expressed (1). These lineage-specific differences in P1 methylation underlie P1 hypomethylation in GC progression (2). Immune cell recruitment triggered *H. pylori* infection (3), leads to altered cell-type composition of the gastric epithelium leading to decreased P1 methylation. Conversely, P2 lacks methylation in both GECs and immune cells, thus its methylation level is unaffected by altered tissue cellularity. In gastric tumours, P2 becomes aberrantly hypermethylated (in concert with other CGI promoters on a global scale) in a subset of highly immortalized/transformed GECs (orange shading), leading to a modest increase in P2 methylation in tumour tissue (4). P2 hypermethylated clones have an *in vitro* growth advantage over non-hypermethylated clones, allowing their preferential expansion during cell line establishment from primary tumour tissue (5), leading to a significant over-representation of P2 hypermethylated clones among GC cell lines (6).